Accepted Manuscript

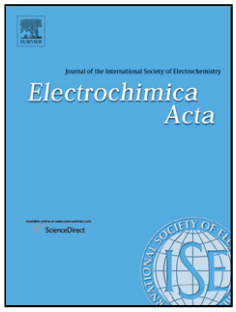

Title: Oxygen electroreduction on carbon-supported Pd nanocubes in acid solutions

Author: Heiki Erikson Madis Lüsi Ave Sarapuu Kaido Tammeveski Jose Solla-Gullón Juan M. Feliu

PII: S0013-4686(15)30900-2
DOI: http://dx.doi.org/doi:10.1016/j.electacta.2015.11.125
Reference: EA 26125

To appear in: *Electrochimica Acta*

Received date: 1-10-2015
Revised date: 19-11-2015
Accepted date: 25-11-2015

Please cite this article as: Heiki Erikson, Madis Lüsi, Ave Sarapuu, Kaido Tammeveski, Jose Solla-Gullón, Juan M.Feliu, Oxygen electroreduction on carbon-supported Pd nanocubes in acid solutions, Electrochimica Acta http://dx.doi.org/10.1016/j.electacta.2015.11.125

This is a PDF file of an unedited manuscript that has been accepted for publication. As a service to our customers we are providing this early version of the manuscript. The manuscript will undergo copyediting, typesetting, and review of the resulting proof before it is published in its final form. Please note that during the production process errors may be discovered which could affect the content, and all legal disclaimers that apply to the journal pertain.

ACCEPTED MANUSCRIPT

Oxygen electroreduction on carbon-supported Pd nanocubes in acid solutions

Heiki Erikson[a], Madis Lüsi[a], Ave Sarapuu[a], Kaido Tammeveski[a,*,1]kaido.tammeveski@ut.ee,

Jose Solla-Gullón[b,1], Juan M. Feliu[b,1]

[a]*Institute of Chemistry, University of Tartu, Ravila 14a, 50411 Tartu, Estonia*

[b]*Instituto de Electroquímica, Universidad de Alicante, Apartado 99, 03080 Alicante, Spain*

[*]Corresponding author: Tel.: +372-7375168; fax: +372-7375181

[1]ISE member

Highlights

- Carbon-supported Pd nanocubes of three different size and loading were prepared
- The specific activity for oxygen reduction reaction is independent of Pd content
- Pd nanocubes possess higher specific activity for ORR than spherical Pd nanoparticles
- The ORR on carbon-supported Pd nanocubes proceed mainly via 4-electron pathway
- Tafel behaviour of ORR on carbon-supported Pd nanocubes is similar to that of bulk Pd

Abstract

The oxygen reduction reaction (ORR) was studied on carbon-supported cubic palladium nanoparticles of different sizes (~30 nm, ~10 nm and ~7 nm). Cetyltrimethylammonium

ACCEPTED MANUSCRIPT

bromide (CTAB) and polyvinylpyrrolidone (PVP) were used as capping agents to prepare the nanocubes and Pd content in the catalyst samples was 20 and 50 wt%. The surface morphology of the prepared materials was studied by transmission electron microscopy (TEM). The catalyst materials were electrochemically characterised by cyclic voltammetry and CO stripping experiments. The rotating disk electrode (RDE) method was employed for ORR studies in 0.5 M H_2SO_4 and 0.1 M $HClO_4$ solutions. The ORR results revealed that the specific activity of cubic Pd nanoparticles is higher than that of spherical Pd particles and does not depend on the Pd content in the catalyst, but decreases with decreasing the size of Pd nanocubes. Mass activity of Pd nanocubes increased with decreasing the particle size. The ORR proceeds mainly via 4-electron pathway and the reaction mechanism is similar to that on bulk Pd.

Keywords: Oxygen reduction; Electrocatalysis; Pd nanoparticles; Pd nanocubes; Supported catalysts

1. Introduction

In recent studies palladium has proven to be good alternative to platinum as catalyst for oxygen reduction reaction (ORR) [1, 2]. Pd has similar properties to Pt as they are in the same group of the periodic table, have the same *fcc* crystal structure and similar atomic size. The main advantage of Pd as compared to Pt is its lower price and higher abundance. It has been shown that Pd single crystal facets have different electrocatalytic activity towards the ORR. Kondo *et al*. showed that, in perchloric acid solution, the activity increases in the following order for the low-index planes: Pd(110) < Pd(111) < Pd(100) [3]. As the surface of cubic Pd particles is mostly composed of Pd(100) facets [4], it is expected that Pd nanocubes would efficiently catalyse the ORR. Indeed, in several studies Pd nanocubes have been prepared and their ORR activity has been evaluated in sulphuric acid [4-7], perchloric acid [7, 8] and in potassium hydroxide [4, 9] solutions. Previously we have shown that cubic Pd nanoparticles (PdNPs) have about three to four times higher specific activity than that of spherical PdNPs in acid [5] and in alkaline media [4]. Shao *et al*. studied approximately 6 nm Pd nanocubes supported on carbon and observed that the specific activity of O_2 reduction in perchloric acid is 10 times higher for Pd nanocubes as compared to octahedral particles [8]. Lee and Chiou demonstrated that in addition to higher activity for ORR, the Pd nanocubes show higher methanol tolerance as compared to spherical PdNPs [6]. Cubic Pd nanoparticles are also efficient catalysts for methanol, ethanol and formic acid oxidation, showing three to four

ACCEPTED MANUSCRIPT

times higher current densities than commercial Pd catalysts [9]. However, Shao *et al*. did not find any advantage of ~5 nm cubic PdNPs for formic acid oxidation, but confirmed the shape dependence of the ORR in sulphuric acid and perchloric acid solutions [7]. Recently, it was reported that palladium concave nanocubes enclosed with high-index facets have superior electrocatalytic activity for methanol oxidation as compared to commercial Pd/C catalyst [10]. In addition to chemically synthesised cubic palladium nanoparticles, triangular Pd rods have been prepared by electrochemical deposition [11]. These particles had mostly Pd(111) planes on the surface and also some Pd(100) and displayed a higher electrocatalytic activity towards the ORR and methanol oxidation as compared to polycrystalline Pd surfaces. A 10-fold increase in specific activity has been observed for ORR on Pd nanorods in perchloric acid solution [12] but the explanation that this is due to the prevalence of Pd(110) crystal facet is in contradiction with the results of single crystal facets [3]. Pd icosahedra with predominant Pd(111) facet have shown high electrocatalytic activity towards the ORR while being ethanol tolerant in alkaline media [13]. The enhanced electrocatalytic properties are suggested to arise not from their crystallographic structure, but from the adsorbed polyallylamine that is used in the synthesis of these Pd particles. Recently, it has been shown that the activity of hydrogen evolution reaction depends on the shape of Pd nanoparticles [14].

Studying the particle size effect is also very important for practical electrocatalysts [15, 16]. In alkaline medium, Jiang *et al*. have observed that specific activity increases three times with increasing particle size from 3 to 16.7 nm. The mass activity increased 1.3 times when particle size increased from 3 to 5 nm, but then decreased with further increasing the particle size [15]. In perchloric acid solution the size effect is more pronounced and the specific activity has a maximum at the Pd nanoparticle size of about 5 to 6 nm, while the mass activity increases with decreasing particle size [16]. It is suggested that the particle size effect arises from several aspects like changes in the distribution of low-index planes on the surface, the relative abundance of low coordination sites and the electronic state of Pd [16].

For practical catalysts it is important to have large surface area for higher efficiency, thus it is important to choose suitable support material for the catalyst. For example, it has been shown that the pre-treatment of carbon support changes the morphology of the catalyst and thus specific activity, mass activity and the amount of hydrogen peroxide produced [17]. By electrodepositing Pd onto nitrogen-doped highly oriented pyrolytic graphite (HOPG) it was observed that there is no advantage over pure HOPG and the stability of Pd on N-doped material was even worse than that on pure HOPG. This was suggested to be due to nitrogen interactions with palladium [18]. However, Jukk *et al*. successfully prepared PdNP/nitrogen-

ACCEPTED MANUSCRIPT

doped graphene composites that exhibited excellent electrocatalytic activity towards the ORR [19]. Pd nanoparticles supported on N-doped ordered mesoporous graphitic carbon nanospheres also showed enhanced electrocatalytic activity and stability, thanks to enriched mesopores, large active surface area and homogeneous nanoparticles distribution [20]. Interestingly, Carrera-Cerratos *et al*. demonstrated that Pd nanocatalysts are more active when reduced graphene oxide is used as support instead of traditional high-area carbon, but for Pt nanoparticles carbon support yielded better results [21]. Huang *et al*. synthesised PdNPs on reduced graphene oxide that showed similar ORR activity to commercial Pt/C catalyst [22].
Recently, we have investigated the kinetics of the ORR on shape-controlled Au nanoparticles supported on carbon [23]. In this study, carbon-supported Pd nanocubes of different size and varied metal loading in the catalyst have been prepared and their electrocatalytic properties towards the oxygen reduction reaction have been evaluated using a rotating disk electrode.

2. Experimental

For the preparation of Pd/C catalysts three methods were used. Pd cubes with the size of ~30 nm were prepared using cetyltrimethylammonium bromide (CTAB) as a capping agent [24], whereas 10 nm and 7 nm Pd nanocubes were synthesised by two methods developed by Xia and co-workers using polyvinylpyrrolidone (PVP) [25, 26].
To prepare 30 nm particles, 10 mL of 10 mM H_2PdCl_4 and 200 mL of 12.5 mM CTAB were mixed together, heated to 95 °C and 1.6 mL of 100 mM ascorbic acid solution was added. The reaction was allowed to proceed for 20 min at 95 °C. After cooling the product was divided into three portions and different amounts of carbon powder (Vulcan XC-72R, Cabot Corp.) were introduced to obtain 20 and 50 wt% catalysts by continuously mixing until getting uniform suspensions. For cleaning the catalysts, some pellets of NaOH were added to the mixture, which was then filtrated and washed several times with water. Finally the sample was dried overnight at 75 °C. These catalysts with 20 and 50 wt% Pd are designated as PdCub1-20 and PdCub1-50, respectively.
In order to prepare ca 10 nm Pd nanocubes on carbon support the appropriate amounts of PVP, K_2PdCl_4, KBr and ascorbic acid were mixed together in water and then heated for 3 h at 80 °C [25], after cooling, carbon powder was added to form 20 wt% catalyst (designated as PdCub2-20). In order to clean the Pd catalyst the procedure suggested by Zalineeva *et al*. was used [14]. Finally the catalyst was filtered, washed several times with water and dried overnight at 75 °C. Pd nanocubes with the size of approximately 7 nm were prepared by using

ACCEPTED MANUSCRIPT

a similar method, but replacing some of the bromide with chloride [26], these catalysts are designated as PdCub3-20.

For comparison, spherical PdNPs supported on carbon were prepared by citrate method [5, 27]. Briefly, Pd precursor K_2PdCl_4 and sodium citrate were mixed together and then ice cold $NaBH_4$ solution was added to produce the Pd nanoparticles. After allowing the reaction to proceed for 15 min the appropriate amount of carbon powder was added to yield 20 wt% Pd/C catalyst, designated as PdSph-20. Then, NaOH was added and suspension was filtered, washed and dried at 75 °C overnight.

In addition to the Pd-based catalysts prepared in this study, commercially available 20 wt% Pd/C catalyst (Premetek Co, USA) was also electrochemically tested.

In order to characterise the prepared catalysts a transmission electron microscope (TEM) (JEM-2010, JEOL) was used. The samples for TEM imaging were prepared by placing a droplet of the Pd/C suspension onto a formvar/carbon coated copper grid and allowing the solvent to evaporate in air at room temperature.

The Pd content in Pd/C samples was evaluated by thermogravimetric analysis (TGA) using a Mettler-Toledo TGA/SDTA851 thermobalance with a temperature ramp of 10 ºC min^{-1} from 25 to 850 ºC in an oxidative atmosphere (N_2:O_2 = 4:1).

The working electrode was prepared by mounting glassy carbon (GC) disks (GC-20SS, Tokai Carbon) with geometric surface area (*A*) of 0.196 cm^2 into Teflon holders. The surface of the electrodes was polished to a mirror finish with 1.0 and 0.3 µm alumina slurries (Buehler). After polishing, the electrodes were sonicated in Milli-Q water (Millipore) for 5 min in order to remove polishing residues. The catalyst ink was prepared by dispersing 1 mg of Pd/C in 1 mL of water, which contained 0.5% of Nafion and 20 µL of this suspension was pipetted onto the GC electrode surface and the solvent was allowed to evaporate at room temperature.

The solutions for electrochemical testing were made from H_2SO_4 (Suprapur, Merck), $HClO_4$ (Sigma-Aldrich) and Milli-Q water. The argon (99.999%), oxygen (99.999%) and carbon monoxide were supplied by AGA. The electrochemical measurements were carried out using a standard three-electrode glass cell with gold wire as counter electrode and reversible hydrogen electrode (RHE) as reference electrode (all potentials in this paper are given with respect to RHE). The potential was applied with an Autolab PGSTAT30 potentiostat/galvanostat controlled with General Purpose Electrochemical System (GPES) software. Prior to the ORR studies the electrodes were electrochemically characterised by cyclic voltammetry (CV) that was carried out in O_2-free 0.5 M H_2SO_4 or 0.1 M $HClO_4$ solution by scanning potential between 0.1 and 0.8 V at a potential scan rate (*v*) of 50 mV s^{-1}.

ACCEPTED MANUSCRIPT

The CO adsorption was done by bubbling CO gas through the solution at 0.1 V until the surface was fully blocked, which was confirmed by the absence of current peaks in the H_{UPD} region, then the CO was removed from the solution by purging with argon for 30 min [28]. The CO stripping was carried out by scanning the potential to upper potential limit of 1 V at 20 mV s^{-1}. The oxygen reduction measurements were performed in O_2-saturated 0.5 M H_2SO_4 and 0.1 M $HClO_4$ solutions by scanning the potential between 0.1 and 0.95 V at 10 mV s^{-1}. For the rotating disk electrode (RDE) experiments, an EDI101 rotator and a CTV101 speed control unit (Radiometer) were employed. The electrode rotation rate (ω) was varied from 360 to 4600 rpm. All experiments were conducted at room temperature (23±1 °C).

3. Results and discussion

3.1. Physical characterisation of Pd/C catalysts

Representative TEM micrographs of cubic Pd nanocatalysts prepared by different methods are presented in Figure 1. It can be seen that the particles are mainly cubic in shape and the side length of the cubes is determined by the synthesis method used. Using CTAB as capping agent, the particles with the size of about 30 nm are obtained (Figures 1a and b), but the methods employing PVP result in smaller particles, ~10 nm and ~7 nm (Figures 1c and d). The spherical PdNPs used for comparison were 2-5 nm in size as revealed from TEM images. It can also be observed that the distribution of Pd on Vulcan carbon XC-72R is rather uniform. Previous studies with Pd nanocubes have shown that the Pd(100) facet is dominant on those particles [4, 27], suggesting that the cubic Pd nanoparticles prepared in this study have the same features.

Thermogravimetric analysis was performed in order to evaluate the real content of palladium in the carbon-supported catalyst materials. The results were in good agreement with the expected values, as the samples PdCub1-20 and PdCub1-50 contained 18 and 55 wt% of Pd, PdCub2-20 18 wt% and PdCub3-20 19 wt% of Pd. The mass of the Pd/C catalysts prepared using CTAB started to decrease sharply at about 500 °C, but for the PdCub2-20 and PdCub3-20 an initial smoother decrease was observed at lower temperatures, which is possibly due to the decomposition of PVP residues left in the catalyst.

3.2 Cyclic voltammetry and CO stripping

Cyclic voltammetry and carbon monoxide adsorption-oxidation experiments were carried out in order to electrochemically characterise Pd/C catalysts. The CO oxidation enables to clean the surface of PtNPs from the impurities retained from the synthesis, it has been shown that

ACCEPTED MANUSCRIPT

this procedure does not affect the shape of Pt nanoparticles [28], this procedure has been also successfully used for Pd nanoparticles [4, 5, 27]. After the CO adsorption, the surface of PdNPs was fully covered by CO, as the hydrogen desorption peaks were absent and there was no current until the start of the oxidation of CO at about 0.85 V (Figure 2a). The CO stripping peaks were positioned between 0.91 and 0.94 V and the adsorbed gas was removed with a single cycle to 1 V. The CO stripping behaviour is in good agreement with the results obtained previously with unsupported Pd nanocubes in sulphuric acid solution [4, 5].

The CV curves of carbon-supported Pd nanocubes in 0.5 M H_2SO_4 after CO stripping experiments are presented in Figure 2b. The shape of these CV curves is similar to those reported previously for Pd nanocubes [4, 5] and to those of Pd(100) single-crystal electrodes with distinctive hydrogen adsorption and desorption peaks [29, 30]. As compared to platinum Pd is less inert as the dissolution takes place at potentials above 0.8 V vs RHE [31]. The topography of bulk polycrystalline Pd has been shown to undergo remarkable changes during surface oxidation [32]. It has been shown recently that in alkaline media, where Pd is more stable, repetitive potential scanning changes the shape of cubic Pd nanoparticles to spherical [33]. Therefore scanning to more positive potentials was avoided in order to prevent the dissolution of Pd and resulting change of the shape and size of the PdNPs. The distinctive peaks observed on cyclic voltammograms at 0.22 and 0.3 V in the H_{UPD} region are characteristic to Pd(100) facet [29]. The CV curves of spherical PdNPs and commercial Pd/C resemble those of bulk polycrystalline Pd [34]. In perchloric acid similar behaviour was observed as in sulphuric acid, with the difference that the H_{UPD} peaks were less well defined.

In order to calculate the real electroactive surface area (A_r) the charge corresponding to the reduction of PdO was found from the CV curves registered between 0.1 and 1.4 V in Ar-saturated acid solution after the ORR measurements, using the value of 424 $\mu C\ cm^{-2}$ as charge density associated with the reduction of a monolayer of PdO [34]. As expected, the electroactive area increased with increasing Pd content and also with decreasing Pd nanocube size (Table 1). The spherical Pd nanoparticles exhibited the highest electroactive surface area due to their smallest size.

3.3. Oxygen reduction reaction studies

After the cyclic voltammetry studies and oxidation of pre-adsorbed carbon monoxide the electrocatalytic activity of the prepared Pd/C catalysts towards the oxygen reduction reaction in O_2-saturated 0.5 M H_2SO_4 and 0.1 M $HClO_4$ solutions was investigated. Only the positive-going potential scans were subjected to further analysis. For all Pd/C catalysts typical single-

ACCEPTED MANUSCRIPT

wave polarisation curves were obtained and a representative set of RDE voltammetry curves are presented in Figure 3a and 3c. The RDE data were subjected to the Koutecky-Levich (K-L) analysis:

$$\frac{1}{j} = \frac{1}{j_k} + \frac{1}{j_d} = -\frac{1}{nFkC_{O_2}^b} - \frac{1}{0.62nFD_{O_2}^{2/3}\nu^{-1/6}C_{O_2}^b\omega^{1/2}} \qquad (1)$$

where j is the measured current density, j_k and j_d are the kinetic and diffusion-limited current densities, respectively, n is the number of electrons transferred per O_2 molecule, k is the rate constant for O_2 reduction, F is Faraday constant (96485 C mol^{-1}), ω is the electrode rotation rate (rad s^{-1}), $C_{O_2}^b$ is the concentration of oxygen in the bulk (1.13×10^{-6} mol cm^{-3}) [35], D_{O_2} is the diffusion coefficient of oxygen (1.8×10^{-5} cm^2 s^{-1}) [35] and ν is the kinematic viscosity of the solution (0.01 cm^2 s^{-1}) [36]. These values of O_2 solubility and diffusion coefficient are given for 0.5 M H_2SO_4. In 0.1 M $HClO_4$ solution $C_{O_2}^b$ = 1.22×10^{-6} mol cm^{-3} and D_{O_2} =1.93×10^{-5} cm^2 s^{-1} were employed [37]. From the K-L plots (Figure 3b, 3d) the number of electrons transferred per O_2 molecule was found (insets of Figure 3b, 3d). In $HClO_4$ solution the value of n was close to 4 for all the Pd/C catalysts studied, indicating that the main product of oxygen reduction is water. In sulphuric acid solution the n value was close to 3.5. The reason why n is lower than 4 might be that the ORR on carbon proceeds via 2-electron pathway but this is probably not the reason as it should be observable also in perchloric acid solution where the value of n was close to 4. It has been also suggested that Nafion coating increases the peroxide yield on Pt catalysts [38]. Recently similar behaviour was observed on Pd catalysts, which also showed decreasing diffusion limiting current plateau with increasing Nafion content [39]. Thus the results here suggest that the used electrolyte in collaboration with Nafion may have a small effect on the number of electrons transferred per O_2 molecule.

By comparing the *j-E* curves of 20 and 50 wt% Pd nanocubes (Figure 4a and 4c) it is obvious that the onset potential and half-wave potential ($E_{1/2}$) of O_2 reduction increase with increasing the Pd content. In addition, the activity of the catalysts depends on the Pd particle size, as smaller particles exhibit higher electroactive surface area. As a result, the $E_{1/2}$ values increase in the following order: PdCub1-20 < PdCub2-20 < PdSph-20 ≈ PdCub3-20 < PdCub1-50. In perchloric acid solution the same trend is observable with the exception of spherical nanoparticles that show the highest $E_{1/2}$, which is expected as different anions have different adsorption strength with different crystal facets. In the case of Pt it has been suggested that (bi)sulphate adsorption strength is different on different single crystal planes [40, 41] and due to the similarities between Pd and Pt a similar behaviour is expected on Pd.

ACCEPTED MANUSCRIPT

In order to compare the electrocatalytic activity of different Pd/C catalysts the specific activities (SA) at 0.85 V were calculated:

$$SA = I_k / A_r \quad (2)$$

where I_k is the kinetic current at a given potential and A_r is the real surface area of Pd. Comparing the effect of Pd loading on catalyst it can be concluded that the SA values are independent of the Pd content, being 0.20 and 0.18 mA cm^{-2} in sulphuric acid and 0.24 and 0.27 mA cm^{-2} in perchloric acid for PdCub1-20 and PdCub1-50, respectively. Comparison of the activities of the Pd nanocubes prepared by different methods (20% Pd/C catalysts) reveals that the samples prepared using CTAB have somewhat higher specific activity than those prepared using PVP (Table 1). This is probably not due to a change in particle size as usually the particle size effect is observed for particles smaller than 10 nm [15, 16]. Also an opposite trend for Pd catalysts has been observed so that the specific activities increase with increasing the particle size [42, 43]. The lower activity may partially come from the fact that the relative proportion of the most active (100) surface facets is lower for smaller nanocubes, due to the effect of truncation. Another reason may be that PVP is not completely removed from the catalysts surface and blocks the active sites of PdNPs from the access of O_2 molecules [44]. When comparing the specific activities in sulphuric acid and perchloric acid then it is evident that the SA values in the latter case are somewhat higher, which can be explained by stronger (bi)sulphate adsorption [45].

Our previous research showed that the spherical PdNPs have about 3-4 times lower specific activity than that of the nanocubes [4, 5]. Similarly in this research, about 2-3 times lower specific activity for spherical PdNPs and commercial Pd/C was observed, which is apparently due to their smallest size and different surface crystallography. Shao *et al*. showed that Pd cubes enclosed with (100) facets were one order of magnitude more active for ORR than Pd octahedra enclosed by (111) facets [8].

The mass activities (MA) were also calculated at 0.85 V:

$$MA = I_k / m_{Pd} \quad (3)$$

where I_k is the kinetic current at a given potential and m_{Pd} is the mass of Pd in the catalyst layer. For all samples prepared using CTAB the MA values were expectedly similar. The active surface area increases with decreasing particle size and thus the mass activity should also increase. As the PdNPs prepared with PVP are smaller, then their MA is higher as compared to PdCub1-20 as predicted. The spherical Pd nanoparticles had the MA value similar to that of smallest cubes in sulphuric acid solution but it was the highest in perchloric

ACCEPTED MANUSCRIPT

acid, which might arise also from the different adsorption strength of anions. This observation suggests that the crystallographic effects are sufficiently bigger to compensate the effect of changing the particle size in sulphuric acid solution.

The Tafel analysis (Figure 4b and 4d) was carried out and a tendency of increasing the Tafel slope value with increasing the loading of Pd nanocubes was in evidence. The Tafel slope values were rather constant in sulphuric acid solution, but in perchloric acid a small change in the slope value was observed. At low current densities the Tafel slope value in perchloric acid solution was near -90 mV but it increased to values above -120 mV at higher current densities (Table 1). In sulphuric acid solution a single Tafel slope value was determined for palladium nanocubes and it was similar to that in perchloric acid at higher current densities. Spherical Pd nanoparticles and commercial Pd/C catalyst had the Tafel slope values about -65 mV that increases to -120 mV at higher current densities. In overall the Tafel slope values in sulphuric acid solution coincide with the values obtained for the same catalyst in perchloric acid solution at high current densities. The Tafel slope values found in this study are somewhat higher than -120 mV that is usually observed for Pd catalysts in acid media [17, 45-48], but also with unsupported Pd nanocubes we have previously observed the slope values up to -150 mV [4]. Similarly, Salvador-Pascual *et al*. have observed one Tafel slope region in sulphuric acid with the value of -120 mV for Pd nanoparticles [49]. However, Alvares *et al*. observed the slope values close to -60 mV and suggested that this corresponds to oxide covered electrodes [50]. Thus, it may be assumed that the carbon-supported Pd nanocubes prepared in this study have lower coverage of oxides than the spherical Pd nanoparticles and the smallest Pd nanocubes, as the Tafel slope value for these was below -120 mV. Similar conclusions were made by Shao *et al*. who observed that the coverage of oxygen-containing species on Pd nanocubes was much lower than on Pd octahedra [8]. Also it may be assumed that the oxide coverage was higher in perchloric acid as at low current densities the Tafel slope value was below -120 mV. Tafel slope values close to -120 mV suggest that the reaction mechanism on cubic Pd nanoparticles supported on carbon is the same as on bulk palladium and the rate-determining step is the transfer of the first electron to O_2 molecule [4, 46, 47].

4. Conclusions

Pd nanocubes of three different particle sizes supported on Vulcan carbon XC-72R were synthesised and their electrocatalytic activity towards the oxygen reduction reaction was compared to that of spherical PdNPs and commercial Pd/C catalyst. The cyclic voltammetry experiments showed characteristic peaks of H_{UPD} on Pd(100) facet that were improved by CO

ACCEPTED MANUSCRIPT

stripping. The oxygen reduction reaction was studied in sulphuric acid solution as well as in perchloric acid. The prepared carbon-supported Pd nanocubes showed higher electrocatalytic activity in perchloric acid solution but the general behavioural tendencies were similar in both solutions. The oxygen reduction studies revealed that the specific activity and mass activity of carbon-supported cubic PdNPs does not depend on metal loading. However, the SA decreases somewhat with decreasing the size of Pd nanocubes and is the smallest for spherical PdNPs and commercial Pd/C catalyst. Mass activities increased uniformly with decreasing the size of cubic Pd nanoparticles. Tafel analysis showed that the mechanism of the ORR on carbon-supported Pd nanocubes is the same as on bulk Pd. The Koutecky-Levich analysis revealed that the ORR proceeds mainly via a four-electron pathway yielding water.

Acknowledgements

This research was financially supported by institutional research funding (IUT20-16) of the Estonian Ministry of Education and Research and by the Estonian Research Council (Grant No. 9323). HE thanks the Archimedes Foundation for scholarship. JMF acknowledges financial support from MINECO (Spain), project CTQ2013-44083-P.

References

[1] E. Antolini, Palladium in fuel cell catalysis, Energy Environ. Sci. 2 (2009) 915.

[2] M. Shao, Palladium-based electrocatalysts for hydrogen oxidation and oxygen reduction reactions, J. Power Sources 196 (2011) 2433.

[3] S. Kondo, M. Nakamura, N. Maki, N. Hoshi, Active sites for the oxygen reduction reaction on the low and high index planes of palladium, J. Phys. Chem. C, 113 (2009) 12625.

[4] H. Erikson, A. Sarapuu, N. Alexeyeva, K. Tammeveski, J. Solla-Gullon, J.M. Feliu, Electrochemical reduction of oxygen on palladium nanocubes in acid and alkaline solutions, Electrochim. Acta 59 (2012) 329.

[5] H. Erikson, A. Sarapuu, K. Tammeveski, J. Solla-Gullon, J.M. Feliu, Enhanced electrocatalytic activity of cubic Pd nanoparticles towards the oxygen reduction reaction in acid media, Electrochem. Commun., 13 (2011) 734.

[6] C.-L. Lee, H.-P. Chiou, Methanol-tolerant Pd nanocubes for catalyzing oxygen reduction reaction in H_2SO_4 electrolyte, Appl. Catal. B 117 (2012) 204.

[7] M.H. Shao, J. Odell, M. Humbert, T.Y. Yu, Y.N. Xia, Electrocatalysis on shape-controlled palladium nanocrystals: oxygen reduction reaction and formic acid oxidation, J. Phys. Chem. C 117 (2013) 4172.

ACCEPTED MANUSCRIPT

[8] M. Shao, T. Yu, J.H. Odell, M. Jin, Y. Xia, Structural dependence of oxygen reduction reaction on palladium nanocrystals, Chem. Commun. 47 (2011) 6566.

[9] N. Arjona, M. Guerra-Balcazar, L. Ortiz-Frade, G. Osorio-Monreal, L. Alvarez-Contreras, J. Ledesma-Garcia, L.G. Arriaga, Electrocatalytic activity of well-defined and homogeneous cubic-shaped Pd nanoparticles, J. Mater. Chem. A 1 (2013) 15524.

[10] X.B. Xie, G.H. Gao, Z.Y. Pan, T.J. Wang, X.Q. Meng, L.T. Cai, Large-scale synthesis of palladium concave nanocubes with high-index facets for sustainable enhanced catalytic performance, Sci. Rep. 5 (2015) 5.

[11] S. Choi, H. Jeong, K.H. Choi, J.Y. Song, J. Kim, Electrodeposition of triangular Pd rod nanostructures and their electrocatalytic and SERS activities, ACS Appl. Mater. Interfaces, 6 (2014) 3002.

[12] L. Xiao, L. Zhuang, Y. Liu, J. Lu, H.D. Abruna, Activating Pd by morphology tailoring for oxygen reduction, J. Am. Chem. Soc. 131 (2009) 602.

[13] G. Fu, X. Jiang, L. Tao, Y. Chen, J. Lin, Y. Zhou, Y. Tang, T. Lu, Polyallylamine functionalized palladium icosahedra: one-pot water-based synthesis and their superior electrocatalytic activity and ethanol tolerant ability in alkaline media, Langmuir 29 (2013) 4413.

[14] A. Zalineeva, S. Baranton, C. Coutanceau, G. Jerkiewicz, Electrochemical behavior of unsupported shaped palladium nanoparticles, Langmuir 31 (2015) 1605.

[15] L. Jiang, A. Hsu, D. Chu, R. Chen, Size-dependent activity of palladium nanoparticles for oxygen electroreduction in alkaline solutions, J. Electrochem. Soc. 156 (2009) B643.

[16] W.J. Zhou, M. Li, O.L. Ding, S.H. Chan, L. Zhang, Y.H. Xue, Pd particle size effects on oxygen electrochemical reduction, Int. J. Hydrogen Energy 39 (2014) 6433.

[17] S.M.S. Kumar, J.S. Herrero, S. Irusta, K. Scott, The effect of pretreatment of Vulcan XC-72R carbon on morphology and electrochemical oxygen reduction kinetics of supported Pd nano-particle in acidic electrolyte, J. Electroanal. Chem. 647 (2010) 211.

[18] W. Ju, M. Favaro, C. Durante, L. Perini, S. Agnoli, O. Schneider, U. Stimming, G. Granozzi, Pd nanoparticles deposited on nitrogen-doped HOPG: new insights into the Pd-catalyzed oxygen reduction reaction, Electrochim. Acta 141 (2014) 89.

[19] K. Jukk, N. Kongi, L. Matisen, T. Kallio, K. Kontturi, K. Tammeveski, Electroreduction of oxygen on palladium nanoparticles supported on nitrogen-doped graphene nanosheets, Electrochim. Acta 137 (2014) 206.

ACCEPTED MANUSCRIPT

[20] D. Ye, R. Zhang, Y. Fu, J. Bu, Y. Wang, B. Liu, J. Kong, Co-calcination-derived Pd budded in N-doped ordered mesoporous graphitic carbon nanospheres for advanced methanol-tolerant oxygen reduction, Electrochim. Acta 160 (2015) 306.

[21] R. Carrera-Cerritos, V. Baglio, A.S. Arico, J. Ledesma-Garcia, M.F. Sgroi, D. Pullini, A.J. Pruna, D.B. Mataix, R. Fuentes-Ramirez, L.G. Arriaga, Improved Pd electro-catalysis for oxygen reduction reaction in direct methanol fuel cell by reduced graphene oxide, Appl. Catal. B 144 (2014) 554.

[22] Y.X. Huang, J.F. Xie, X. Zhang, L. Xiong, H.Q. Yu, Reduced graphene oxide supported palladium nanoparticles via photoassisted citrate reduction for enhanced electrocatalytic activities, ACS Appl. Mater. Interfaces, 6 (2014) 15795.

[23] H. Erikson, A. Sarapuu, K. Tammeveski, J. Solla-Gullon, J.M. Feliu, Shape-dependent electrocatalysis: oxygen reduction on carbon-supported gold nanoparticles, ChemElectroChem 1 (2014) 1338.

[24] W. Niu, Z.-Y. Li, L. Shi, X. Liu, H. Li, S. Han, J. Chen, G. Xu, Seed-mediated growth of nearly monodisperse palladium nanocubes with controllable sizes, Cryst. Growth Des. 8 (2008) 4440.

[25] B. Lim, M.J. Jiang, J. Tao, P.H.C. Camargo, Y.M. Zhu, Y.N. Xia, Shape-controlled synthesis of pd nanocrystals in aqueous solutions, Adv. Funct. Mater. 19 (2009) 189.

[26] M.S. Jin, H.Y. Liu, H. Zhang, Z.X. Xie, J.Y. Liu, Y.N. Xia, Synthesis of Pd nanocrystals enclosed by {100} facets and with sizes < 10 nm for application in CO oxidation, Nano Res. 4 (2011) 83.

[27] F.J. Vidal-Iglesias, R.M. Aran-Ais, J. Solla-Gullon, E. Garnier, E. Herrero, A. Aldaz, J.M. Feliu, Shape-dependent electrocatalysis: formic acid electrooxidation on cubic Pd nanoparticles, Phys. Chem. Chem. Phys. 14 (2012) 10258.

[28] J. Solla-Gullon, V. Montiel, A. Aldaz, J. Clavilier, Electrochemical characterisation of platinum nanoparticles prepared by microemulsion: how to clean them without loss of crystalline surface structure, J. Electroanal. Chem. 491 (2000) 69.

[29] N. Hoshi, K. Kagaya, Y. Hori, Voltammograms of the single-crystal electrodes of palladium in aqueous sulfuric acid electrolyte: Pd(S)-n(111)x(111) and Pd(S)-n(100)x(111), J. Electroanal. Chem. 485 (2000) 55.

[30] N. Hoshi, M. Kuroda, Y. Hori, Voltammograms of stepped and kinked stepped surfaces of palladium: Pd(S)-n(111)x(100) and Pd(S)-n(100)x(110), J. Electroanal. Chem. 521 (2002) 155.

[31] L.D. Burke, J.K. Casey, An examination of the electrochemical behavior of palladium

ACCEPTED MANUSCRIPT

electrodes in acid, J. Electrochem. Soc. 140 (1993) 1284.

[32] I. Srejic, Z. Rakocevic, M. Nenadovic, S. Strbac, Oxygen reduction on polycrystalline palladium in acid and alkaline solutions: topographical and chemical Pd surface changes, Electrochim. Acta 169 (2015) 22.

[33] A. Zadick, L. Dubau, A. Zalineeva, C. Coutanceau, M. Chatenet, When cubic nanoparticles get spherical: an identical location transmission electron microscopy case study with Pd in alkaline media, Electrochem. Commun. 48 (2014) 1.

[34] M. Grden, M. Lukaszewski, G. Jerkiewicz, A. Czerwinski, Electrochemical behaviour of palladium electrode: oxidation, electrodissolution and ionic adsorption, Electrochim. Acta 53 (2008) 7583.

[35] S. Gottesfeld, I.D. Raistrick, S. Srinivasan, oxygen reduction kinetics on a platinum RDE coated with a recast nafion film, J. Electrochem. Soc. 134 (1987) 1455.

[36] D.R. Lide, CRC handbook of chemistry and physics, CRC Press, Boca Raton, 2001.

[37] R.R. Adzic, J. Wang, B.M. Ocko, Structure of metal adlayers during the course of electrocatalytic reactions: O_2 reduction on Au(111) with Tl adlayers in acid solutions, Electrochim. Acta 40 (1995) 83.

[38] H. Yano, E. Higuchi, H. Uchida, M. Watanabe, Temperature dependence of oxygen reduction activity at Nafion-coated bulk Pt and Pt/carbon black catalysts, J. Phys. Chem. B 110 (2006) 16544.

[39] M. Goral-Kurbiel, A. Drelinkiewicz, R. Kosydar, J. Gurgul, B. Dembinska, P.J. Kulesza, The effect of Nafion ionomer on electroactivity of palladium-polypyrrole catalysts for oxygen reduction reaction, J. Solid State Electrochem. 18 (2014) 639.

[40] M.D. Macia, J.M. Campina, E. Herrero, J.M. Feliu, On the kinetics of oxygen reduction on platinum stepped surfaces in acidic media, J. Electroanal. Chem. 564 (2004) 141.

[41] A. Kuzume, E. Herrero, J.M. Feliu, Oxygen reduction on stepped platinum surfaces in acidic media, J. Electroanal. Chem. 599 (2007) 333.

[42] W. Ju, T. Bruelle, M. Favaro, L. Perini, C. Durante, O. Schneider, U. Stimming, Palladium nanoparticles supported on highly oriented pyrolytic graphite: preparation, reactivity and stability, ChemElectroChem 2 (2015) 547.

[43] A. Anastasopoulos, J.C. Davies, L. Hannah, B.E. Hayden, C.E. Lee, C. Milhano, C. Mormiche, L. Offin, The particle size dependence of the oxygen reduction reaction for carbon-supported platinum and palladium, ChemSusChem 6 (2013) 1973.

ACCEPTED MANUSCRIPT

[44] N. Naresh, F.G.S. Wasim, B.P. Ladewig, M. Neergat, Removal of surfactant and capping agent from Pd nanocubes (Pd-NCs) using tert-butylamine: its effect on electrochemical characteristics, J. Mater. Chem. A 1 (2013) 8553.

[45] A. Sarapuu, A. Kasikov, N. Wong, C.A. Lucas, G. Sedghi, R.J. Nichols, K. Tammeveski, Electroreduction of oxygen on gold-supported nanostructured palladium films in acid solutions, Electrochim. Acta 55 (2010) 6768.

[46] L.M. Vracar, D.B. Sepa, A. Damjanovic, Palladium electrode in oxygen-saturated aqueous-solutions - reduction of oxygen in the activation-controlled region, J. Electrochem. Soc. 133 (1986) 1835.

[47] L.M. Vracar, D.B. Sepa, A. Damjanovic, Palladium electrode in oxygen-saturated aqueous-solutions – potential dependent adsorption of oxygen containing species and their effect on oxygen reduction, J. Electrochem. Soc. 136 (1989) 1973.

[48] H. Erikson, A. Kasikov, C. Johans, K. Kontturi, K. Tammeveski, A. Sarapuu, Oxygen reduction on Nafion-coated thin-film palladium electrodes, J. Electroanal. Chem. 652 (2011) 1.

[49] J.J. Salvador-Pascual, S. Citalan-Cigarroa, O. Solorza-Feria, Kinetics of oxygen reduction reaction on nanosized Pd electrocatalyst in acid media, J. Power Sources 172 (2007) 229.

[50] G.F. Alvarez, M. Mamlouk, S.M.S. Kumar, K. Scott, Preparation and characterisation of carbon-supported palladium nanoparticles for oxygen reduction in low temperature PEM fuel cells, J. Appl. Electrochem. 41 (2011) 925.

Figure captions

Figure 1. TEM images of Pd nanocubes on carbon support (a) PdCub1-20, (b) PdCub1-50, (c) PdCub2-20 and (d) PdCub3-20.

Figure 2. (a) Electro-oxidation of pre-adsorbed CO and (b) cyclic voltammograms of carbon supported Pd nanocubes in Ar-saturated 0.5 M H_2SO_4. (a) v = 10 mV s^{-1} and (b) 50 mV s^{-1}. Current densities are normalised to the real surface area of electrocatalysts.

ACCEPTED MANUSCRIPT

Figure 3. A set of RDE voltammetry curves for oxygen reduction on (a) PdCub1-50 in O_2-saturated 0.5 M H_2SO_4 solution and (c) PdCub3-20 in O_2-saturated 0.1 M $HClO_4$ solution; (b,d) the corresponding Koutecky-Levich plots; insets show the potential dependence of *n*. *v* = 10 mV s^{-1}. Current densities are normalised to the geometric area of GC.

Figure 4. Comparison of RDE voltammetry curves for oxygen reduction on Pd/C catalysts in O_2-saturated 0.5 M H_2SO_4 (a) and 0.1 M $HClO_4$ (c) and the corresponding Tafel plots (b,d). ω = 1900 rpm, *v* = 10 mV s^{-1}. Current densities are normalised to the geometric area of GC.

Table 1. Kinetic parameters for oxygen reduction on Pd/C catalysts in 0.1 M H_2SO_4 and 0.1 M $HClO_4$. ω = 1900 rpm.

		0.5 M H_2SO_4				0.1 M $HClO_4$			
Catalyst	A_r (cm^2)	Tafel slope* (mV)	$E_{1/2}$ (V)	SA at 0.85 V (mA cm^{-2})	MA at 0.85 V (A g^{-1})	Tafel slope* (mV)	$E_{1/2}$ (V)	SA at 0.85 V (mA cm^{-2})	MA at 0.85 V (A g^{-1})
PdCub1-20	0.22	-139	0.61	0.20	12	-136	0.65	0.24	26
PdCub1-50	0.73	-147	0.71	0.18	11	-140	0.74	0.27	21
PdCub2-20	0.43	-125	0.64	0.12	14	-138	0.69	0.18	28
PdCub3-20	0.49	-119	0.67	0.13	17	-120	0.69	0.16	29
PdSph-20	1.07	-126	0.66	0.08	16	-124	0.77	0.12	37
commercial Pd/C	0.54	-120	0.58	0.04	12	-124	0.78	0.13	34

*Tafel slopes at high current densities.

ACCEPTED MANUSCRIPT

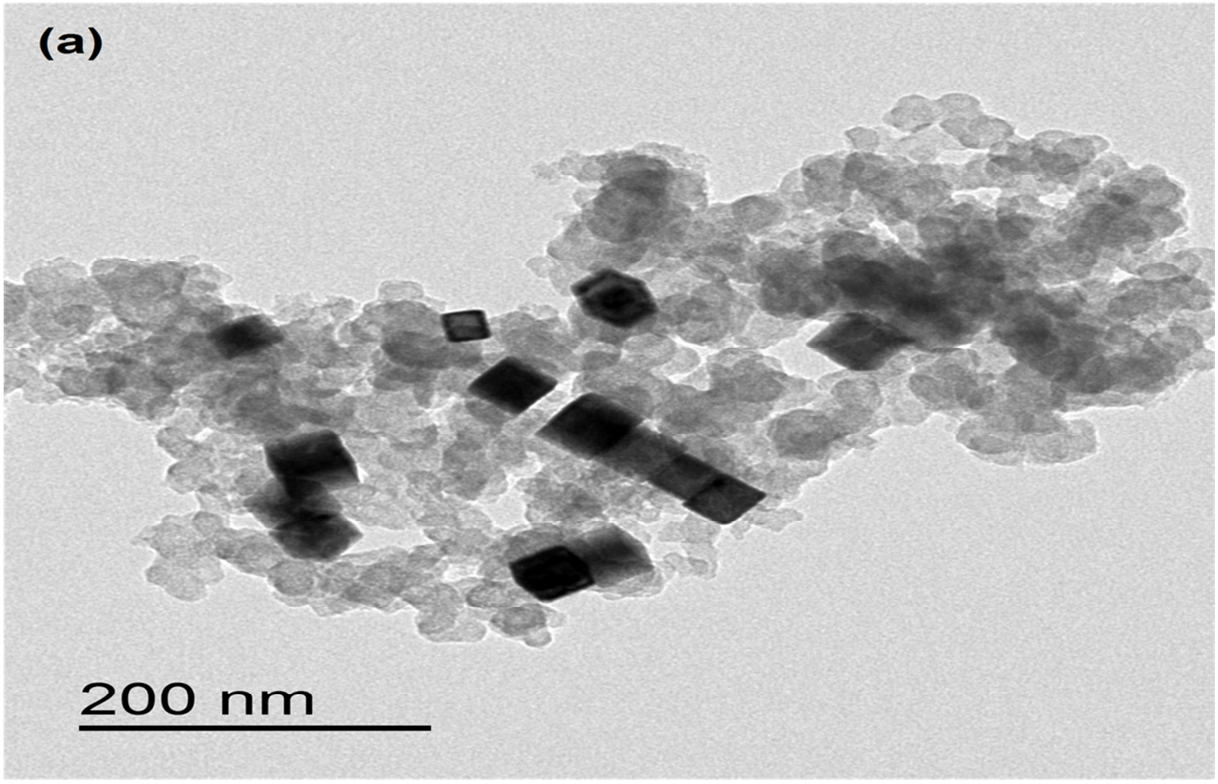

Figure1a .

ACCEPTED MANUSCRIPT

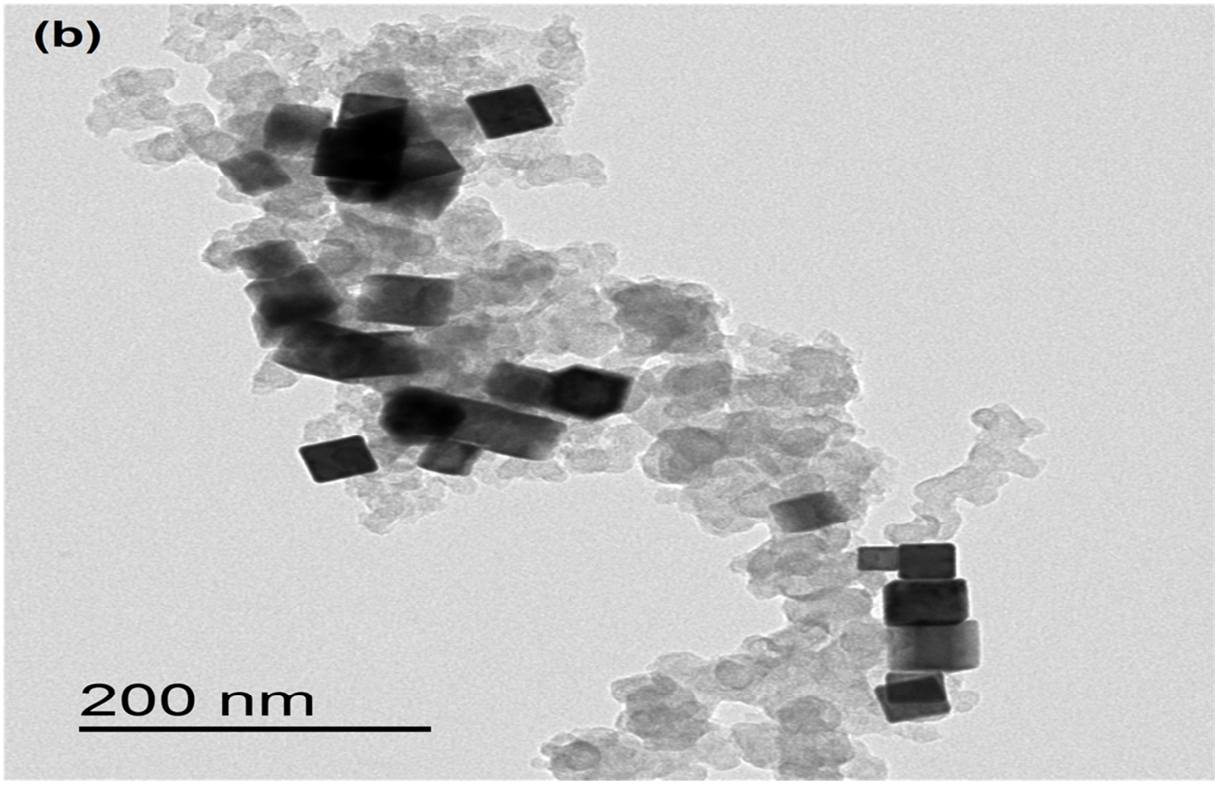

Figure1b .

ACCEPTED MANUSCRIPT

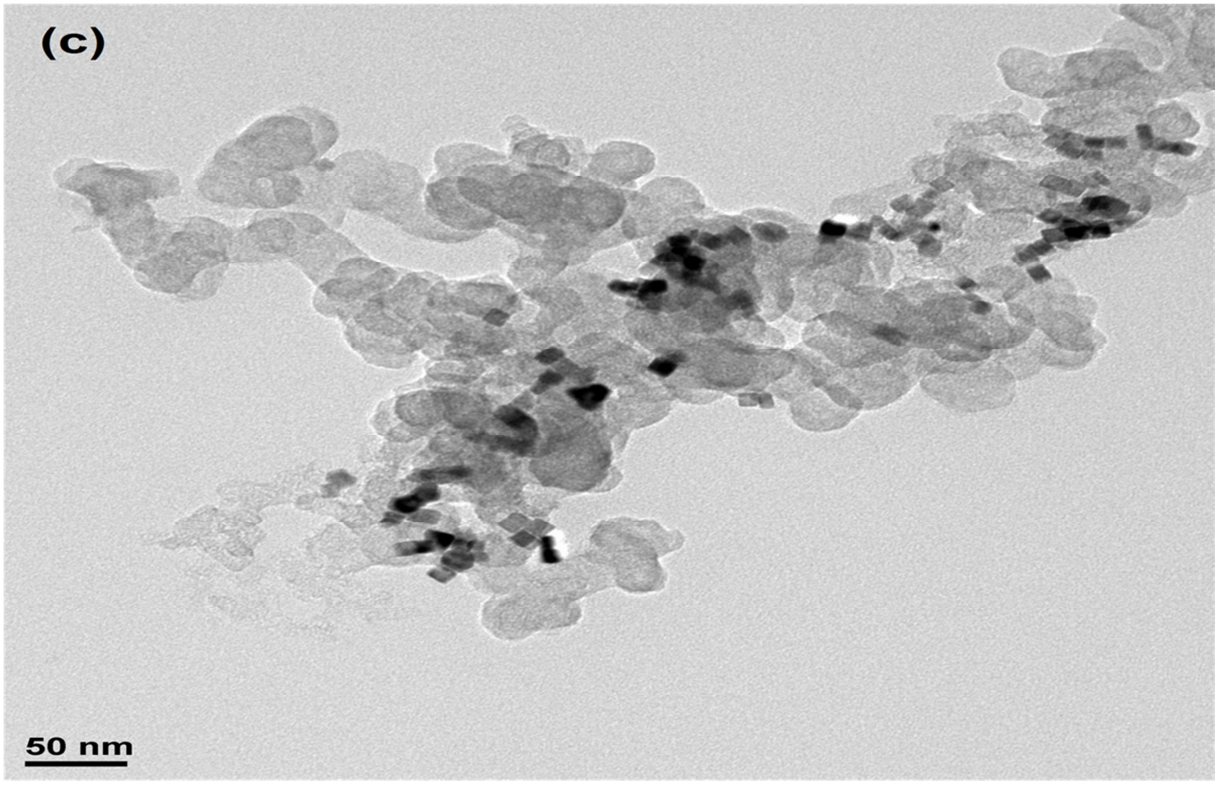

Figure1c .

ACCEPTED MANUSCRIPT

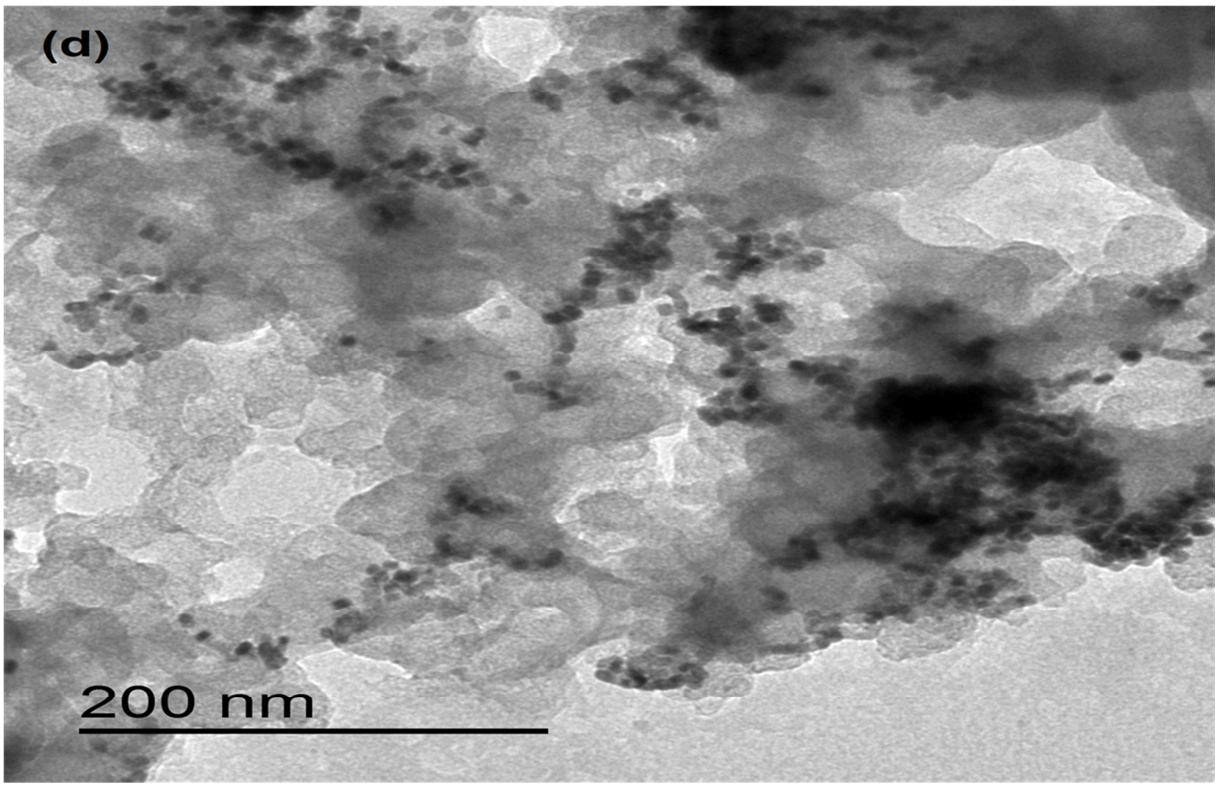

Figure1d .

ACCEPTED MANUSCRIPT

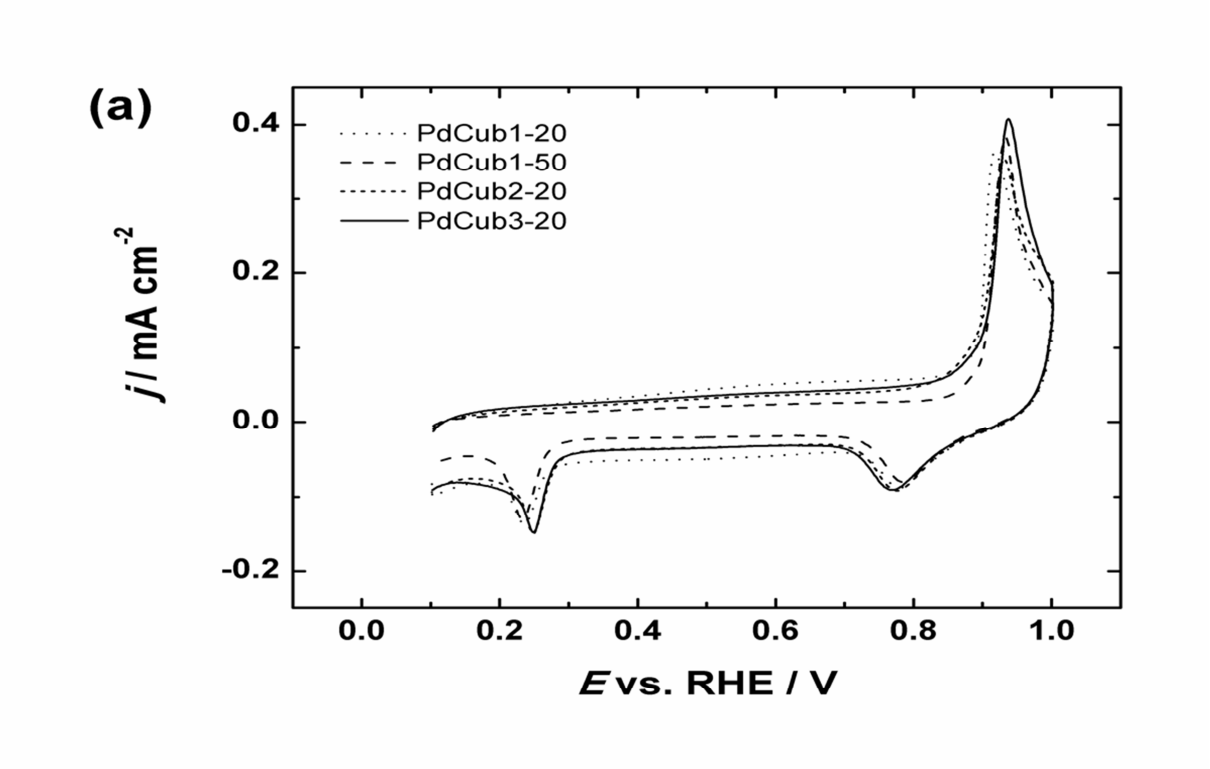

Figure2a .

ACCEPTED MANUSCRIPT

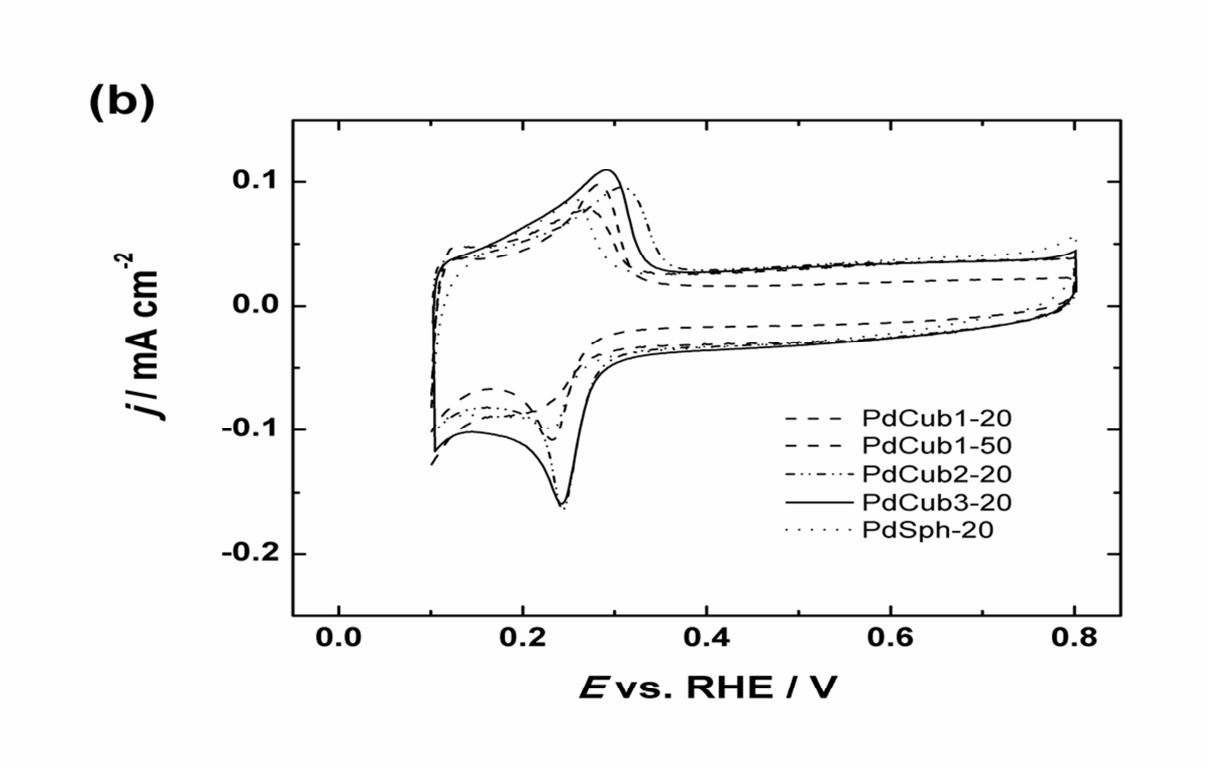

Figure2b .

ACCEPTED MANUSCRIPT

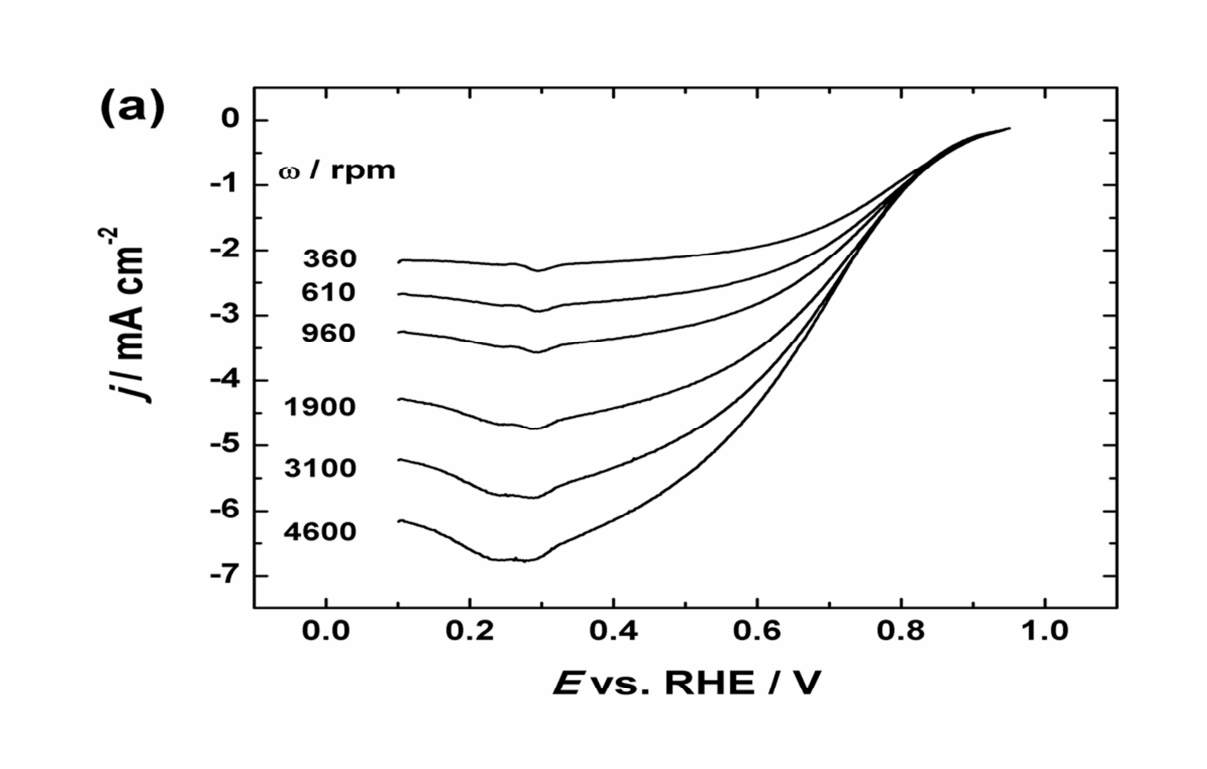

Figure3a .

ACCEPTED MANUSCRIPT

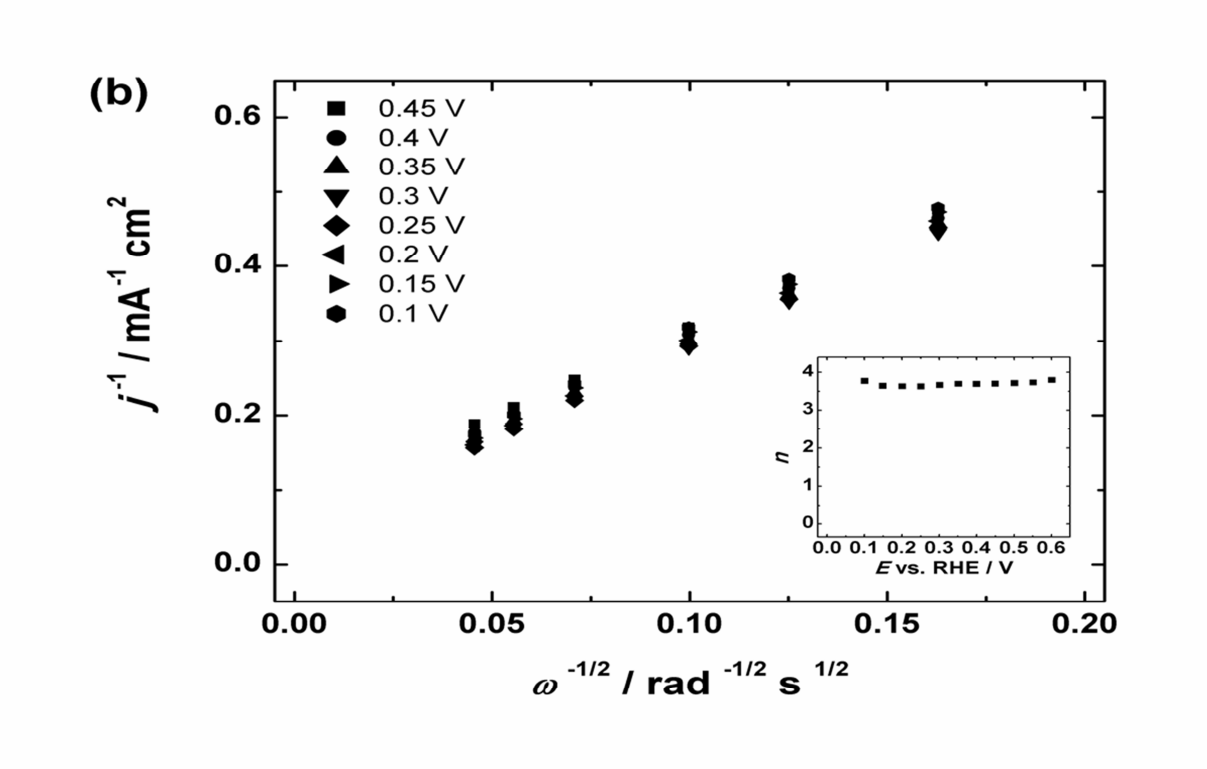

Figure3b .

ACCEPTED MANUSCRIPT

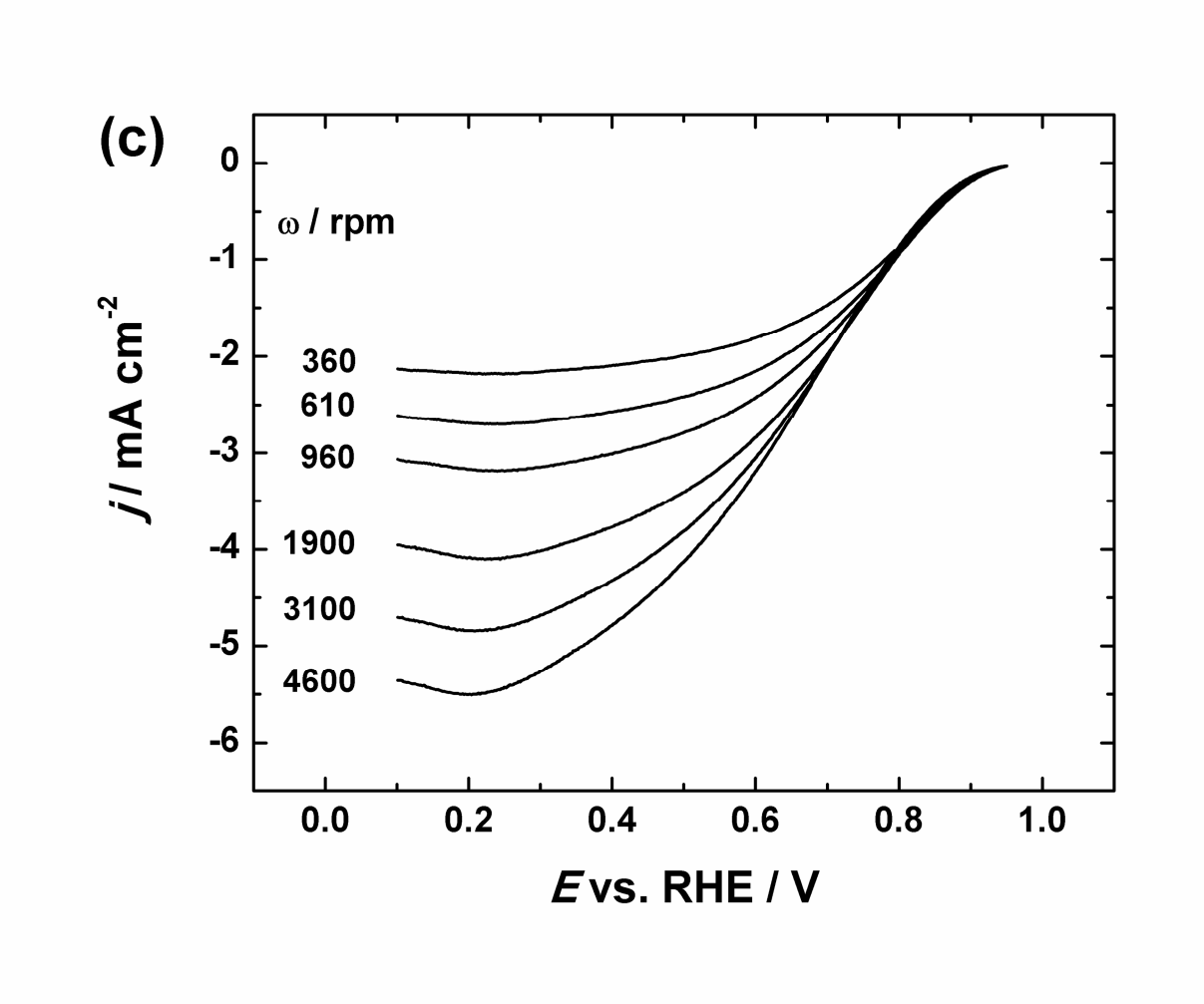

Figure3c .

ACCEPTED MANUSCRIPT

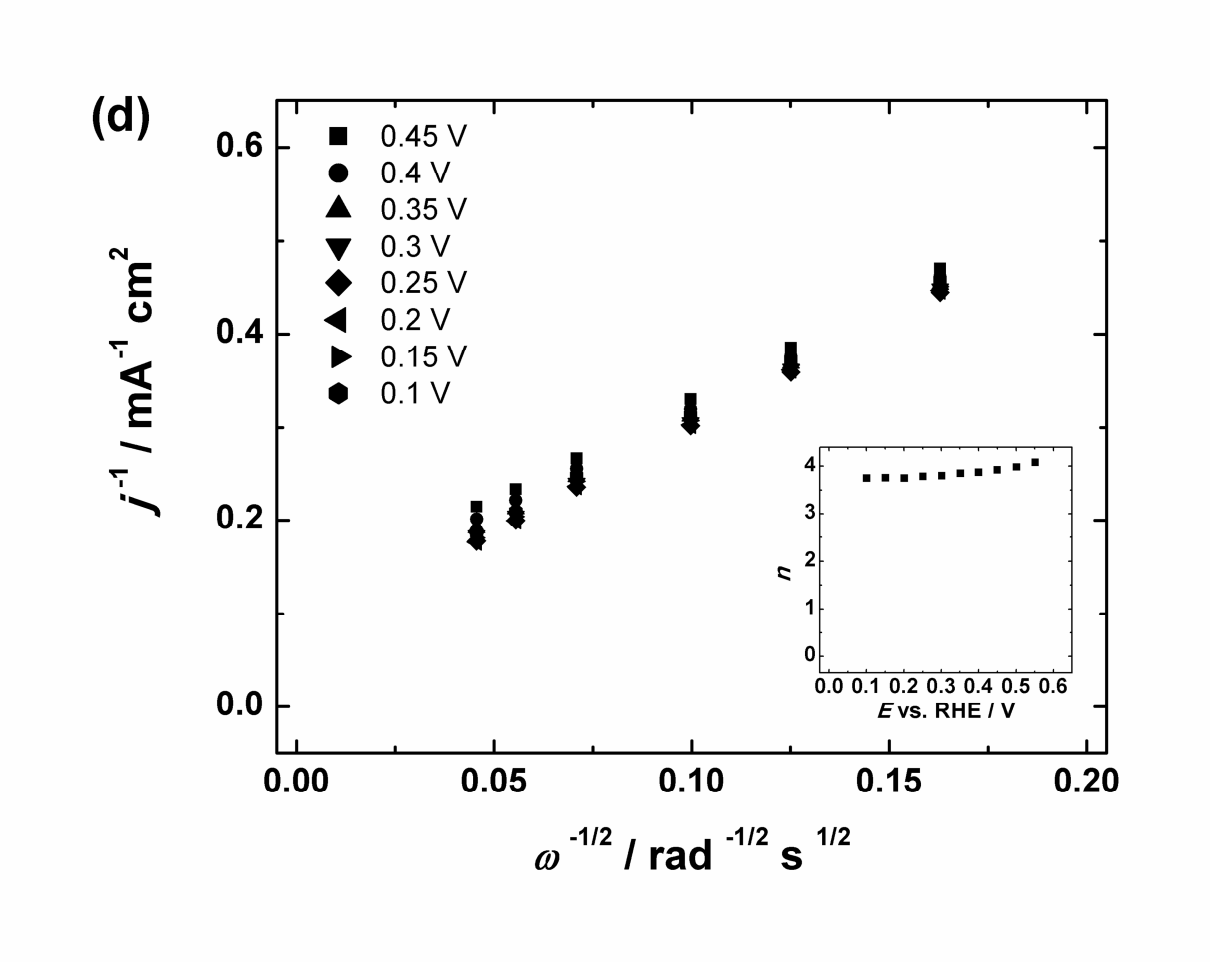

Figure3d .

ACCEPTED MANUSCRIPT

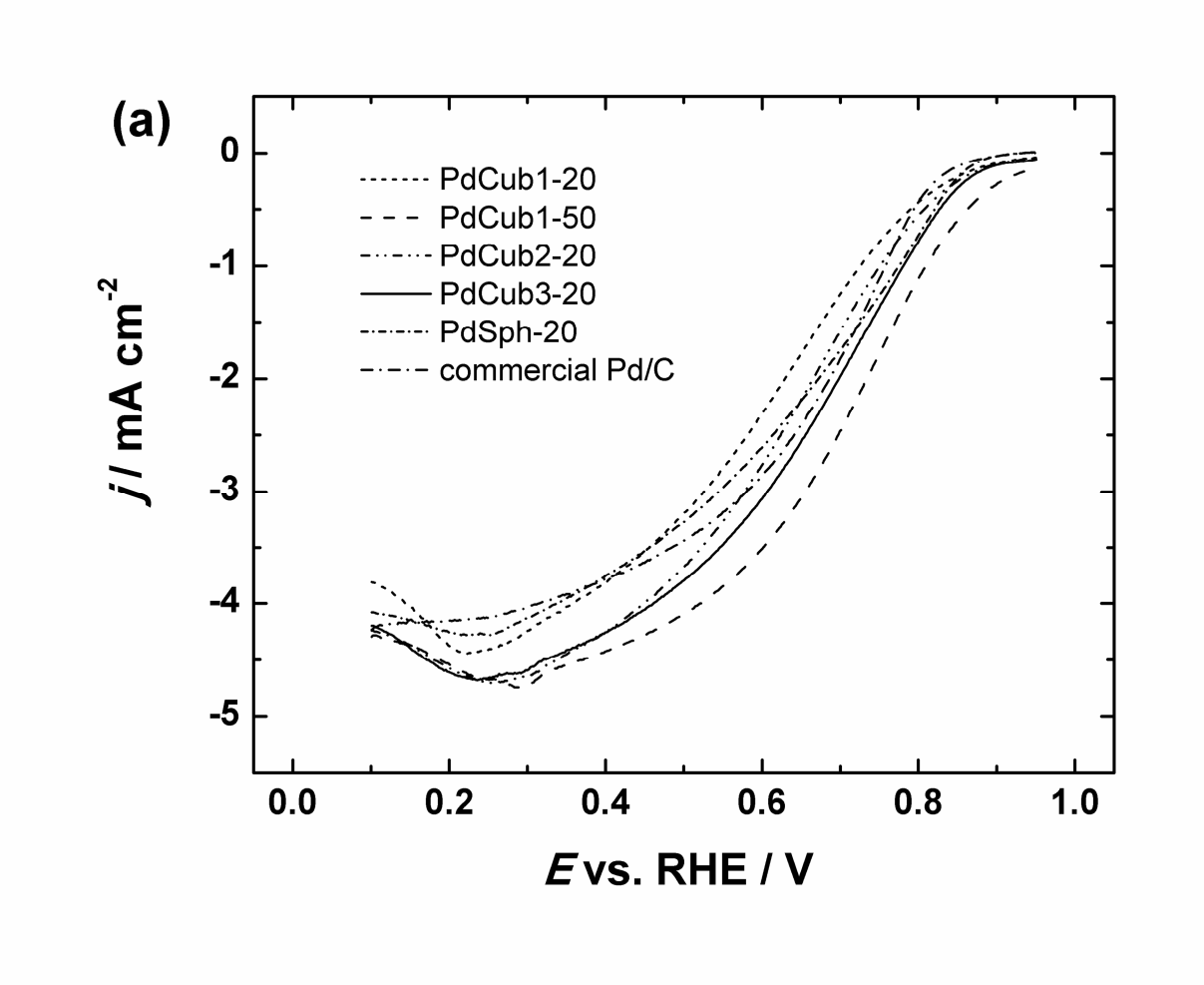

Figure4a .

ACCEPTED MANUSCRIPT

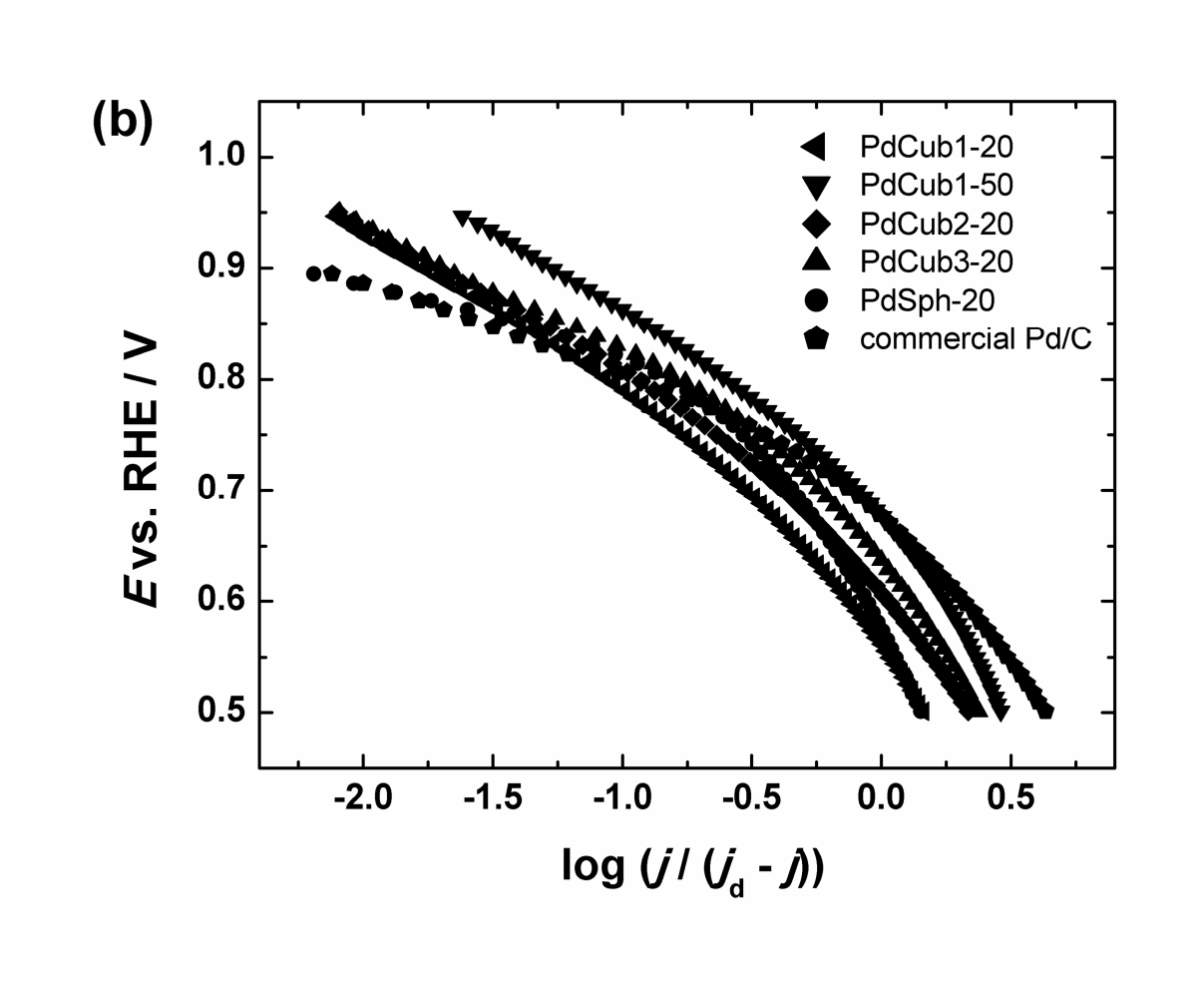

Figure4b .

ACCEPTED MANUSCRIPT

Figure4c .

ACCEPTED MANUSCRIPT

Figure4d .